Title: The Amino Terminus of Tau Inhibits Kinesin-Dependent Axonal Transport: Implications for Filament Toxicity

Abbreviated Title: Tau filaments inhibit kinesin-based motility.

Authors and Affiliations: Nichole E. LaPointe[1,3 ‡], Gerardo Morfini[2,3,‡*], Gustavo Pigino[2,3], Irina N. Gaisina[4], Alan P. Kozikowski[4], Lester I. Binder[1], and Scott T. Brady[2,3]

[1]Department of Cell and Molecular Biology, Feinberg School of Medicine, Northwestern University, 303 E. Chicago Ave., Chicago, IL 60611, [2]Department of Anatomy and Cell Biology, University of Illinois at Chicago, Chicago, IL 60612, [3]Marine Biological Laboratory, Woods Hole, MA 02543, USA, [4]Drug Discovery Program, Department of Medicinal Chemistry and Pharmacognosy, University of Illinois at Chicago, Chicago, IL 60612

[‡:] These authors contributed equally to this work,

Corresponding Authors:

Drs. Scott Brady and Gerardo Morfini

University of Illinois at Chicago

Dept. of Anatomy and Cell Biology MC512

808 S Wood St

Chicago, IL 60612 USA

Phone (312) 996-6791

Fax (312) 413-0354

stbrady@uic.edu

gmorfini@uic.edu

10 Figures, 0 Tables
Number of pages:

Keywords: Alzheimer's disease/axonal transport/ tau filament/GSK3/PP1/kinesin/tau

Acknowledgements: The authors would like to thank Natalia Marangoni, Sarah Pollema, Kelly Monk and Hannah Brown for assistance with axoplasm experiments, and Dr. Athena Andreadis for the Tau6P and Tau6D constructs. Special thanks to Dr. Angela Guillozet-Bongaarts for a critical reading of the manuscript. Research supported by NIH awards NS049834 (N.E.L.), AG14453 (L.I.B.), NINDS grants NS23868, NS23320, NS41170 and NS43408 (S.B.), MDA (S.B.), ALSA (G.M, S.B), and HDSA (G.M.).

ABSTRACT

The neuropathology of Alzheimer's disease (AD) and other tauopathies is characterized by filamentous deposits of the microtubule-associated protein tau, but the relationship between tau polymerization and neurotoxicity is unknown. Here, we examined effects of filamentous tau on fast axonal transport (FAT) using isolated squid axoplasm. Monomeric and filamentous forms of recombinant human tau were perfused in axoplasm, and their effects on kinesin- and dynein-dependent FAT rates evaluated by video microscopy. While perfusion of monomeric tau at physiological concentrations showed no effect, tau filaments at the same concentrations selectively inhibited anterograde (kinesin-dependent) FAT, triggering the release of conventional kinesin from axoplasmic vesicles. Pharmacological experiments indicated that the effect of tau filaments on FAT is mediated by protein phosphatase 1 (PP1) and glycogen synthase kinase-3 (GSK-3) activities. Moreover, deletion analysis suggested that these effects depend on a conserved 18-amino acid sequence at the amino terminus of tau. Interestingly, monomeric tau isoforms lacking the C-terminal half of the molecule (including the microtubule binding region) recapitulated the effects of full-length filamentous tau. Our results suggest that pathological tau aggregation contributes to neurodegeneration by altering a regulatory pathway for FAT.

INTRODUCTION

Tau is a microtubule-associated protein (MAP) involved in microtubule dynamics and maintenance (Amos and Schlieper 2005), and insoluble filamentous tau aggregates form in Alzheimer's disease (AD) and several other neurodegenerative tauopathies (reviewed in (Gamblin et al. 2003a). Despite the strong positive correlation between the appearance of filamentous tau and neuronal dysfunction (reviewed in (Binder et al. 2005)), no toxic mechanism has been directly tied to these structures, and as a result the toxicity of tau filaments remains a subject of debate (King 2005).

In AD, degenerating neurons exhibit alterations in synaptic function (Bell and Claudio Cuello 2006; Yoshiyama et al. 2007), the appearance of neuritic varicosities, and the mislocalization of various membrane-bound organelles (MBOs), all of which indicate that intracellular transport is disrupted in this disease (reviewed in (Morfini et al. 2002a). Given these observations, and the central role of tau in AD pathology, a number of investigators have explored the effects of monomeric tau on microtubule-dependent fast axonal transport (FAT). Although reports have been published arguing both for (Ebneth et al. 1998; Seitz et al. 2002; Vershinin et al. 2007), and against (Morfini et al. 2007a) the idea that high levels of soluble tau can reduce anterograde FAT by interfering with the attachment of the molecular motor kinesin, there is no evidence that such levels of tau are seen in normal or pathological neurons. Remarkably, even though the hallmark of AD and other tauopathies is the presence of intracellular tau filaments, the biological effects of filamentous tau on FAT have not been assessed previously.

In this paper, we examined the effects of tau filaments on FAT using isolated squid axoplasm. Whereas at low, physiologically relevant, ratios of tau to tubulin, monomeric tau has

no effect, tau filaments selectively inhibit anterograde, conventional kinesin-dependent fast axonal transport (FAT). Furthermore, deletion experiments indicate that this effect requires the first 18 a.a. at the amino terminus of tau, which becomes abnormally exposed upon polymerization. Consistent with this notion, monomeric tau isoforms lacking the microtubule-binding region (MTBR) and the C-terminus mimicked the effect of tau filaments on FAT. Finally, we show that tau filaments do not act at the microtubule surface, but rather inhibit anterograde FAT by activating protein phosphatase 1 (PP1) and glycogen synthase kinase 3 (GSK-3). Taken together, our findings reveal a novel gain-of-function mechanism by which the formation of tau filaments may play a critical role in AD pathogenesis.

MATERIALS AND METHODS

Reagents: CREBpp was synthesized and purified (95%) by New England Peptide (Gardner, MA). Inhibitor-2 (I-2), SB203580, and okadaic acid were purchased from Calbiochem (San Diego, CA). Arachidonic acid (AA; Cayman Chemical, Ann Arbor, MI) was stored at -20°C, and working solutions were prepared in 100% ethanol immediately prior to use. Mammalian protease inhibitor cocktail was from Sigma (St. Louis, MO). ING-135 was synthesized as described previously (Kozikowski et al. 2007).

***Recombinant Proteins*:** The full-length tau used in this study (hTau40) corresponds to the longest isoform in adult human brain, containing 441 amino acids and four microtubule-binding repeats (MTBRs). K23 is a tau construct lacking both alternatively-spliced N-terminal exons as well as all four MTBRs. Tau6D and Tau6P are tau isoforms lacking the MTBR region and the C-terminus of canonical tau. The alternative splicing that generates these isoforms occurs in exon 6, and introduces a unique 11 amino acid sequence followed by a stop codon. The specific 11

amino acids vary depending on whether the splice site is proximal or distal to the beginning of exon 6 (Luo et al. 2004). Tau6D and Tau6P isoforms were generated by restriction digestion and ligation of constructs previously described (Luo et al. 2004) and hTau40 (Carmel et al. 1996; Gustke et al. 1994). All other constructs used in this study have been described elsewhere:, Δ2-18 (Gamblin et al. 2003b), 1-421 (Gamblin et al. 2003c), K23 (Preuss et al. 1997). All proteins were expressed in E. coli and purified by means of an N-terminal poly-histidine tag (Abraha et al. 2000; Carmel et al. 1996).

Immunoblots: Tau constructs were spotted onto nitrocellulose membranes (1 ng/μL, 1 μL per spot), blocked with 5% non-fat dry milk in Tris-buffered saline, pH 7.4, and probed with the monoclonal antibodies Tau12 (2 ng/mL), Tau5 (20 ng/mL), and Tau46.1 (20 ng/mL), which recognize amino acids 9-18, 210-230, and 428-441, respectively (Carmel et al. 1996; Ghoshal et al. 2002; Kosik et al. 1988). Primary antibody binding was detected with HRP-conjugated anti-mouse secondary antibody (Vector Laboratories, Burlingame, CA) and ECL developing solution (GE Healthcare, Amersham, UK).

Microtubule-binding Assays: Squid optic lobes were dissected and flash frozen in liquid nitrogen (Morfini et al. 2007a). 1.5 grams of freshly thawed squid optic lobes was homogenized in 2.5 mL of BRB80 buffer (80 mM Pipes, 1 mM $MgCl_2$ and 1 mM EGTA) and 1/100 mammalian protease inhibitor cocktail (Sigma, St. Louis, MO), plus phosphatase and kinase inhibitors (Calbiochem, San Diego, CA) as follows: 1/200 phosphatase inhibitor cocktail II, 200 mM sodium orthovanadate, 200 nM mycrocystin RR, 50 nM okadaic acid, 100 nM K252a, 100 nM staurosporine. Squid optic lobe homogenate was prepared at 4^0C using a glass Dounce homogeneizer. This homogenate was centrifuged at 12,500 x g for 20 min at 4^0C. The supernatant fraction was transferred to a new tube, and centrifuged at 125,000 x g for 5 min at

4^0C in a TL100.3 rotor (Beckman, Fullerton, CA). The supernantant (cytosol) was transferred to a new tube, adjusted to 20 μM taxol, and incubated at 37^0 C for 15 min to allow for microtubule polymerization. After this step, 200 μL aliquots of microtubule-containing cytosol were incubated alone, or with htau40, or K23 tau constructs (5 μM final concentration) for 20 min at 37^0 C. Samples were loaded on top of a 60 μL BRB80 buffer plus 20% sucrose cushion and 20 μM taxol using 1.5 mL microcentrifuge tubes, and centrifuged for 5 min at 125,000 x g at 4^0C using a TLA100.3 rotor (Beckman, Fullerton, CA). Microtubule pellets were resuspended in 200 μL of BRB80. Pellets and supernatant fractions were adjusted to 1X gel loading buffer (GLB) using a 5X GLB stock (0.35 M Tris-HCl pH 6.8, 10% w/v SDS (Sequanal grade, Pierce, Rockford, IL), 36% glycerol, 5% ß-mercaptoethanol, 0.01% bromophenol blue). Membranes were also probed with an antibody against tubulin (DM1a, Sigma) to demonstrate the presence of microtubules in the pellet samples.

Tau Polymerization: Tau polymerization was induced using arachidonic acid as previously described (King et al. 1999), except that KCl was substituted for NaCl in the polymerization buffer. This substitution did not prevent filament formation (see Fig. 5b-d). Briefly, tau protein (4 μM) was incubated at room temperature in reaction buffer (50 mM HEPES, pH 7.6, 50 mM KCl, 5 mM DTT) in the presence of 75 μM arachidonic acid (in ethanol vehicle). Samples of soluble tau were prepared for perfusion in the same manner, except that arachidonic acid was excluded from the polymerization buffer. Control mixtures containing AA but lacking tau were prepared in parallel. Final ethanol concentration in all samples was 3.8%.

Electron Microscopy: Polymerization reactions were allowed to proceed for six hours, fixed with 2% glutaraldehyde, spotted onto 300 mesh formvar/carbon coated copper grids (Electron Microscopy Sciences, Hatfield, PA), and negatively stained with 2% uranyl acetate (King et al.

1999). Samples were examined using a JEOL JEM-1220 electron microscope at 60kV and 12,000X magnification, and photographs were taken using a MegaScan 794/20 digital camera and DigitalMicrograph software version 3.9.3 (Gatan, Pleasanton, CA).

Squid Axoplasm Motility Assays: Axoplasm from squid giant axons (*Loligo pealii*; Marine Biological Laboratory, Woods Hole, MA) was extruded as previously described (Brady et al. 1985). All proteins and inhibitors were diluted in ATP-supplemented X/2 buffer (175 mM potassium aspartate, 65 mM taurine, 35 mM betaine, 25 mM glycine, 10 mM HEPES, 6.5 mM $MgCl_2$, 5 mM EGTA, 1.5 mM $CaCl_2$, 0.5 mM glucose, pH 7.2) for perfusion. For experiments involving tau and their controls, reaction mixtures (containing tau alone, tau and AA, and AA alone) were diluted 1:1 in ATP-supplemented X/2 buffer (final tau concentration 2 μM, when present). Motility was analyzed using a Zeiss Axiomat microscope equipped with a 100X, 1.3 N.A. objective and DIC optics. Organelle velocities were measured by matching calibrated cursor movements to the speed of vesicles moving in the axoplasm (Morfini et al. 2006).

Purification of membrane vesicle fractions from squid axoplasms: Two "sister" axoplasms were prepared from the same animal and incubated with the appropriate effectors (control buffer, active GSK-3β, monomeric tau or filamentous tau) as for motility assays in X/2 buffer plus 1 mM ATP in 25 μL final volume. Active GSK-3β was from Sigma (# G1663). After 40 min incubation, axoplasms were transferred, along with perfusion buffer, to low protein binding 1.5 mL centrifuge tubes containing 200 μL of homogenization buffer [0.25 mM sucrose, 1 mM EDTA, 10 mM Hepes, pH 7.4, 1/100 protease inhibitor cocktail (Sigma #P8340), 1/200 phosphatase inhibitor cocktail set II (Calbiochem # 524627), 2 μM K252a (Calbiochem # 420298), 1 μM PKI (Upstate # 12-151)], and carefully homogenized by 2 passages through a

23G syringe needle and 5 passages through a 27G syringe needle using a 1 mL Hamilton pipette. Axoplasm homogenates were adjusted to 30% iodixanol by mixing 200 μL of axoplasm homogenates with 300 μL of solution D (50% (w/v) iodixanol, 10 mM $MgCl_2$ in 250 mM sucrose). A 500 μL layer of solution E (25% (w/v) iodixanol, 10 mM $MgCl_2$ in 250 mM sucrose) and a 100 μL layer of solution F (5% (w/v) iodixanol, 10 mM $MgCl_2$ in 250 mM sucrose) were loaded on top of the axoplasm homogenates. Samples were centrifuged at 250,000 x g max for 1 hour at 4^0C in an RP55-S Sorvall rotor. 300 μL containing floating vesicles were collected from immediately below the 5% iodixanol interface, and 60 μl of 6X loading sample buffer added. In separate experiments, 0.1% Triton X-100 was added to the axoplasm homogenates prior to centrifugation to confirm the membranous nature of this fraction. Immunoblots were developed using antibodies against kinesin-1 heavy chain (H2, Pfister et al, 1989), dynein intermediate chain (rabbit polyclonal V3, a generous gift from Kevin Vaughan) and SNAP-25 (Synaptic Systems #111-002). Quantitative immunoblotting was performed as described before (Morfini et al, 2006).

Statistical Analysis.

All experiments were repeated at least 3 times. Unless otherwise stated, the data was analyzed by ANOVA followed by post-hoc Student-Newman-Keul's test in order to make all possible comparisons. Comparison of transport data from axoplasm under different conditions was done using a two sample t-test of μ1-μ2 with Datadesk statistical software (Data Description, Inc; Ithaca, NY). Data was expressed as mean ± s.e.m. and significance was assessed at p values as noted.

RESULTS

To evaluate the effect of tau on microtubule-dependent FAT, we used vesicle motility assays in isolated squid axoplasm. In this experimental system, the bi-directional transport of membrane-bound organelles (MBOs) can be directly observed by video-enhanced differential interference contrast (DIC) microscopy. This preparation preserves the ionic strength and complex environment of the cell, and because the axoplasm is isolated from the cell body, nuclear effects can be ignored (Brady et al. 1985). Also, the absence of plasma membrane in this preparation allows for the introduction of experimental agents at tightly controlled concentrations (Morfini et al. 2007a). This system was instrumental in the original discovery of kinesin-1 (Brady 1985), novel regulatory pathways for FAT (Morfini et al. 2006; Morfini et al. 2004; Morfini et al. 2002b), and axonal-specific phosphorylation events (Grant et al. 1999).

Monomeric hTau40 binds to squid microtubules, but does not affect FAT.

Alternative splicing produces six major tau isoforms in the adult human central nervous system. In a previous study, we assayed monomeric tau constructs derived from the shortest tau isoform (352 a.a., hTau23) and established their effects on FAT (Morfini et al. 2007a). In the present study, we chose to use the longest isoform (441 a.a., hTau40), because of its greater propensity to form filaments (Gamblin et al. 2003a). Unlike hTau23, hTau40 contains two alternatively-spliced N-terminal exons (E2 and E3) and four microtubule binding repeats (R1-R4). A schematic of each tau construct used in the present study is shown in Fig. 1a.

Previously, we demonstrated that monomeric hTau23 binds to axonal squid microtubules (Morfini et al. 2007a). To rule out species-related artifacts, we assayed the ability of monomeric hTau40 to interact with endogenous squid microtubules. Microtubule-enriched fractions from squid optic lobe were prepared in the presence or absence of hTau40. Following taxol-induced

microtubule assembly, microtubules and associated proteins were sedimented by centrifugation, and the resulting fractions (supernatants and microtubule-enriched pellets) probed with anti-tau antibodies. A tau construct with low binding affinity (K23) was assayed in parallel to control for non-specific sedimentation. As observed previously (Morfini et al. 2007a), most K23 remained in the supernatant fraction. In contrast, hTau40 was depleted from the supernatant fraction and found in association with the microtubule-enriched pellet fraction (Fig. 1b), indicating that monomeric hTau40 can bind to endogenous squid microtubules.

Microtubule rigidity is increased when tau binds to the microtubule surface, and this effect is observable even at low, non-saturating tau concentrations (Felgner et al. 1997; Morfini et al. 2007a). As an additional indicator of hTau40's ability to interact with squid microtubules, we perfused axoplasm with tau and then examined the morphology of microtubules at the axoplasm periphery. In the absence of exogenous tau, many of these microtubules exhibited a curved appearance (Fig. 2a). However, perfusion of monomeric hTau40 (2 μM) caused peripheral microtubules to acquire a straight, rigid appearance (Fig. 2b), consistent with binding of hTau40 to the microtubule surface (Morfini et al. 2007a). Together with the sedimentation assay, these results demonstrate that hTau40 is capable of binding to squid microtubules.

We next examined the effects of monomeric hTau40 on FAT. We perfused axoplasm with hTau40 at 2 μM, which is within the physiological range for neurons (2-5 μM) (Drubin et al. 1985). The concentration of tubulin in squid axoplasm is 50 μM (Morris and Lasek 1984), resulting in a tau to tubulin ratio of approximately 1:25. FAT rates measured between 30 and 50 min post-perfusion were pooled and compared to axoplasms perfused with control buffer alone. As observed for other monomeric tau constructs (Morfini et al. 2007a), perfusion of hTau40 at 2 μM showed no effect on either anterograde or retrograde FAT (Fig. 3a), demonstrating that

physiological levels of monomeric hTau40 do not impair FAT in this system.

Perfusion of filamentous tau selectively inhibits anterograde FAT.

Recombinant hTau40 forms filaments *in vitro* when incubated with arachidonic acid (reviewed in (Gamblin et al. 2003a)), and these filaments are morphologically similar to those isolated from Alzheimer's disease neuronal tissue (King et al. 1999). To determine the effects of filamentous tau on FAT, we perfused hTau40 filaments (2 μM) into squid axoplasm and monitored anterograde and retrograde FAT rates. Unlike monomeric tau, hTau40 filaments inhibited anterograde, kinesin-dependent FAT rates (Fig. 3b, $p \leq 0.001$) when perfused at the same concentration as monomeric hTau40 (2μM). Perfusion of axoplasms with polymerization buffer alone (see Materials and Methods) had no effect on FAT (data not shown), demonstrating that the effects on FAT were due to the presence of filamentous tau. Significantly, retrograde FAT rates remained unaffected, suggesting that the effects of hTau40 filaments on anterograde FAT were not due to alterations in microtubule integrity. Supporting this idea, htau40 filaments (2 μM) did not produce changes in microtubule morphology when perfused into axoplasm, which also suggests that filamentous tau does not bind to microtubules (Fig. 2c). Similarly, perfusion of equivalent amounts of polymerization buffer (containing arachidonic acid, but no tau) had no effect on FAT (not shown).

The effect of tau filaments on FAT depends upon the extreme N-terminus of tau

Several studies suggest important functional roles for both the amino and carboxy terminus of tau (Amadoro et al. 2006; Amadoro et al. 2004; Brandt et al. 1995; Lee 2005), and the study of selected modifications of these domains constitutes an emerging area of interest in AD (Gamblin et al. 2003c; Guillozet-Bongaarts et al. 2005). To determine whether these domains are involved in FAT inhibition, we assayed two tau constructs, Δ2-18 and 1-421,

containing deletions at the extreme amino- and carboxy-terminus, respectively (see Fig. 1a and Fig. 4a). These deletions do not normally prevent tau from forming filaments (Berry et al. 2003; Gamblin et al. 2003b). However, the buffer conditions required for axoplasm perfusion (see Materials and Methods) differ from the buffer used in previous tau assembly assays. This led us to evaluate the formation of tau filaments under these experimental conditions using electron microscopic analysis. As shown in Fig. 4b-d, hTau40, Δ2-18 and 1-421 all form morphologically undistinguishable filaments under these buffer conditions (Fig. 4b-d).

We then evaluated the effects of Δ2-18 and 1-421 filaments on FAT. Axoplasms perfused with monomeric hTau40 (2 μM) were used as an experimental control, because this treatment results in FAT rates that are indistinguishable from control buffer alone (see Fig. 3a). Filaments composed of hTau40 (hTau40 F) and 1-421 (1-421 F) significantly reduced anterograde FAT rates, compared to hTau40 monomer (hTau40 M; *$p \leq 0.0001$ by a two-sample t test). In contrast, Δ2-18 filaments (Δ2-18 F) had no effect on FAT (Fig. 5a). Retrograde transport was unaffected in all conditions (Fig. 5b). These results suggest that the first 18 a.a. of tau are necessary for the inhibitory effect of tau filaments on anterograde FAT. Although the magnitude of the 1-421 filament effect was not as great that of hTau40 filaments in the time period under analysis, the pattern of inhibition was similar (see Supplemental Fig. 1A) and the effect of 1-421filaments was not significantly different from full-length hTau40 filaments in a t-test. It remains to be determined if the apparent difference is the result of variability in the effective concentration of the two types of filaments, or if some small difference in the structure of the 1-421 filaments affects the presentation of the N-terminus.

Monomeric tau constructs lacking the C-terminal half of the protein recapitulate the effects of tau filaments on FAT.

Results from deletion experiments above suggested that the first 18 a.a. at the amino terminus of tau are required to elicit the inhibitory effect of tau filaments on FAT. However, various full-length tau constructs including the amino terminal 18 a.a. domain do not affect FAT when perfused in monomeric, soluble form (Fig 2 and (Morfini et al. 2007a)), suggesting this domain is abnormally exposed in filamentous hTau40. Supporting this idea, biochemical studies identified a intramolecular interaction between the amino and C-terminus of monomeric tau constructs (Horowitz et al. 2006; Jeganathan et al. 2006). These observations led us to evaluate the effect of endogenous tau isoforms lacking the C-terminal half of the protein on FAT. These isoforms, Tau6P and Tau6D, are the products of two cryptic splice sites in exon 6 (see Fig. 1a). They are identical to canonical tau from amino acids 1-144, at which point splicing introduces a unique 11 amino acid sequence followed by a stop codon. The specific 11 amino acids differ depending on whether the splice site is proximal or distal to the beginning of exon 6 (Luo et al. 2004). Tau6P and Tau6D terminate prior to the MTBR region, and so are not expected to interact with microtubules (Lee et al. 1989) or form filaments (Abraha et al. 2000; von Bergen et al. 2000). When axoplasm was perfused with monomeric Tau6P or Tau6D (2 μM), anterograde FAT was inhibited ($p \leq 0.0001$), but retrograde transport remained unchanged. Since the effects of these two isoforms were indistinguishable, data from Tau6P and Tau6D were pooled (Fig. 6). The inhibitory effect of these tau isoforms was indistinguishable from that of hTau40 filaments, indicating that the amino terminus of tau is sufficient to trigger FAT inhibition (see Discussion).

The effects of tau filaments on FAT are mediated by GSK-3 activity.

The effect of tau filaments and monomeric 6P/6D tau isoforms on anterograde FAT raised questions about the underlying molecular mechanisms. The effect of tau filaments on FAT is unlikely to be due to steric hindrance of kinesin by tau at the microtubule surface,

because filamentous tau is not expected to bind to microtubules (Fig. 2C) and Tau6P/6D isoforms lack a MTBR domain. Instead, we suspected that FAT inhibition might occur through one of the signaling pathways that regulate the activity of the major anterograde motor in this system, conventional kinesin

Several axonal kinases have been identified that play a role in regulating conventional kinesin-dependent FAT, including JNK (Morfini et al. 2006), and GSK-3 (Morfini et al. 2002b) kinases. JNK phosphorylates kinesin heavy chains (KHCs), which inhibits kinesin-1 binding to microtubules and results in reduced anterograde FAT (Morfini et al. 2006). The effects of abnormal JNK activation can be blocked by SB203580 (Morfini et al. 2006), a pharmacological inhibitor that acts on JNK2/3 and other members of the stress-activated protein kinase (SAPK)/JNK family (Coffey et al. 2002; Morfini et al. 2006). To determine whether tau filaments inhibit anterograde FAT through a mechanism involving JNK activation, we co-perfused tau filaments with SB203580 (5 μM). Co-perfusion of tau filaments with SB203580 did not block the effect of tau filaments on FAT (Fig. 7c; different from soluble tau at $p \leq 0.001$), indicating this effect is independent of JNK and other SAPK/JNK kinases (i.e., p38s).

To evaluate whether tau filaments inhibit anterograde FAT through a mechanism involving GSK-3 activation, we co-perfused hTau40 filaments (2 μM) with cAMP response element-binding protein phosphopeptide (CREBpp; 0.5 mM). While many kinases phosphorylate intact CREB protein, the peptide fragment employed here (KRREILSRRPpSYR) is selectively phosphorylated by GSK-3, and therefore acts as a competitive inhibitor of other GSK-3 substrates (Wang et al. 1994b). Perfusion of CREBpp in squid axoplasm alone has no effect on FAT, although it effectively blocks the effects of active GSK-3 on kinesin-1-based motility (Morfini et al. 2004; Morfini et al. 2002b). Remarkably, co-perfusion of tau filaments

and CREBpp blocked tau filament-induced effects on FAT (Fig. 7a), suggesting that the effects of the filaments are dependent on GSK-3 activation. CREBpp also blocked the effects of 1-421 tau filaments, indicating that these filaments act through the same mechanism as filaments of full-length hTau40 (see Supplemental Figure 1).

To confirm that GSK-3 activity is required for tau filaments to inhibit kinesin-dependent FAT, we co-perfused tau filaments with the lithium mimetic ING-135 (100 nM), a highly specific inhibitor of GSK-3 (Kozikowski et al. 2007) (for the structure of this compound in complex with GSK-3β, see Supplemental Figure 2). As with CREBpp, co-perfusion with ING-135 blocked the effect of tau filaments (Fig. 7b), and perfusion of ING-135 alone had no effect on FAT (data not shown). Together, these results suggest that the effect of tau filaments on anterograde FAT involves activation of axonal GSK-3.

Phosphorylation of kinesin light chains (KLCs) by GSK-3 triggers the chaperone-dependent dissociation of kinesin-1 from its cargo (Morfini et al. 2002b; Pigino et al. 2003). To determine whether tau filaments induce the dissociation of kinesin-1 from cargo, we obtained "sister" axoplasms from individual animals and treated them with monomeric or filamentous hTau40 (2 μM). For comparison, we treated other axoplasm pairs with control buffer or with recombinant, active GSK-3β. After 40 min of incubation, we isolated axoplasmic vesicle fractions and evaluated kinesin-1 levels with an antibody against kinesin heavy chains (KHCs). Antibodies recognizing the synaptic integral membrane protein SNAP-25 served as a control for equal vesicle protein loading. The recovery of SNAP-25, kinesin-1 and dynein from vesicles was blocked by addition of 0.1% Triton X-100 to axoplasm homogenates prior to centrifugation, confirming the membranous nature of this fraction (not shown). Perfusion of either filamentous tau or active GSK-3β resulted in ≈50% decrease in the amount of kinesin-1 associated with

vesicles relative to monomeric tau or control buffer, respectively ($p \leq 0.05$ for filamentous tau). In contrast, levels of dynein intermediate chain were unaffected (Fig. 8). These results demonstrate that both tau filaments and GSK-3 selectively inhibit anterograde FAT by leading to dissociation of conventional kinesin-1, but not dynein, from its transported vesicular cargo.

PP1 activity mediates the inhibitory effect of tau filaments on FAT

GSK-3 is inactive when phosphorylated (Wang et al. 1994a), and can be activated by axonal phosphatases (Morfini et al. 2004; Wang et al. 1994a). This prompted us to evaluate whether the inhibitory effects of tau filaments involve the activity of axoplasmic phosphatases. To this end, we co-perfused axoplasm with tau filaments and okadaic acid (100 nM). Okadaic acid inhibits two major serine-threonine phosphatases, namely protein phosphatase 1 (PP1) and protein phosphatase 2A (PP2A). Concentrations of okadaic acid alone up to 1 μM have no effect on FAT (Bloom et al. 1993). Remarkably, okadaic acid blocked the effect of tau filaments on FAT (Fig. 9a), suggesting that tau filament-mediated inhibition of anterograde FAT involves the activity of a major serine-threonine phosphatase. To distinguish between PP1 and PP2A activity, we co-perfused filaments with 50 nM inhibitor-2 (I-2). I-2 selectively inhibits PP1, but has no effect on PP2A, even at micromolar concentrations (Cohen 1991). When co-perfused with tau filaments, I-2 prevented FAT inhibition (Fig. 9b), suggesting that axonal PP1 activity mediates the effect of tau filaments on FAT.

DISCUSSION

We have demonstrated that hTau40 filaments selectively impair anterograde FAT in isolated axoplasm, whereas monomeric hTau40 has no effect at the same concentration. Our results provide a novel link between tau aggregation and neuronal dysfunction, and identify a

specific gain of function mechanism conferred by the aggregation process. Further, our studies suggest that inhibition of kinesin-1-based motility represents an important pathogenic event in AD and other tauopathies.

We have previously described a signaling pathway that regulates conventional kinesin-based motility. In this pathway, increased PP1 activity results in the dephosphorylation and activation of axonal GSK-3 (Morfini et al. 2004). Activated GSK-3 phosphorylates kinesin light chains (KLCs), prompting a chaperone-dependent dissociation of kinesin-1 and cargo (Morfini et al. 2004; Morfini et al. 2002b). Results presented here suggest that tau filaments inhibit anterograde FAT by triggering this pathway (Fig. 10). It is possible that tau filaments directly activate PP1 in this cascade, since tau reportedly binds to PP1 and stimulates its activity (Liao et al. 1998). However, more work is necessary to determine whether tau filaments act directly on PP1, or if additional intermediate components remain undiscovered. Additionally, some feedback from GSK-3 is conceivable, since GSK-3 is a major tau kinase that can also bind directly to tau (Sun et al. 2002), and is reported to be abnormally activated in AD (Ferrer et al. 2005).

We demonstrated that the inhibitory effect of tau filaments on FAT requires the extreme amino terminus of the protein. A pivotal role for this part of the protein is consistent with studies in other experimental systems. For example, overexpression of tau amino terminus induces cell death in cultured neurons through a mechanism involving abnormal kinase activity (Amadoro et al. 2006; Amadoro et al. 2004), and expression of the N-terminus of tau induced microtubule disassembly in cells exposed to beta-amyloid (King et al. 2006). Immunological studies indicate that loss of the N-terminus is an early event in the maturation of tau fibrillar lesions in AD (Horowitz et al. 2004). Our results suggest that such cleavage events may modulate the toxicity

of filamentous tau on FAT. The amino terminus is also the site of AD-related phosphorylation (Lee et al. 2004) and nitration (Reynolds et al. 2006) events, and of the FTDP-17-associated mutations R5L (Poorkaj et al. 2002) and R5H (Hayashi et al. 2002). Analysis of how these modifications influence the effects of tau filaments on FAT may provide further insights into disease progression.

Although hTau40 monomer had no effect on FAT at the concentrations tested, monomers of Tau6P and Tau6D inhibited anterograde FAT as effectively as hTau40 filaments. This result demonstrates that the N-terminus of tau is sufficient to produce the observed effects on FAT, since these isoforms lack the MTBR region and the C-terminal tail of canonical tau. Additionally, it raises the question of why hTau40 monomer failed to show the same inhibitory effect, even though it contains an intact amino terminus. Although monomeric hTau40 was first thought to exist in an extended conformation (Schweers et al. 1994; Syme et al. 2002), recent evidence suggests that tau in solution adopts a globally folded conformation in which the N-terminus folds in close proximity to the C-terminus (Horowitz et al. 2006; Jeganathan et al. 2006). It is possible that this conformation shields the extreme amino terminus, thus preventing hTau40 monomer from inhibiting FAT. In this scenario, polymerization would freeze hTau40 in a different conformation in which the N-terminus is exposed.

With these results, tau joins a growing list of proteins whose pathogenic forms alter regulatory pathways for FAT. Like tau filaments, AD-associated mutations in presenilin-1 inhibit kinesin-1-based motility through GSK-3 activation (Pigino et al. 2003), whereas pathogenic forms of androgen receptor and huntingtin inhibit kinesin-1 dependent transport through JNK activation (Morfini et al. 2006). The current study suggests that AD represents an example of a dysferopathy, where alterations in FAT lead to a dying back neuropathy (Morfini et

al. 2007b), providing further evidence that alterations in regulatory pathways for FAT represent a common pathogenic event in multiple, otherwise apparently unrelated neurodegenerative diseases (Morfini et al. 2002a; Morfini et al. 2005).

REFERENCES

Abraha A, Ghoshal N, Gamblin TC, Cryns V, Berry RW, Kuret J, Binder LI. 2000. C-terminal inhibition of tau assembly in vitro and in Alzheimer's disease. J Cell Sci 113:3737-3745.

Amadoro G, Ciotti MT, Costanzi M, Cestari V, Calissano P, Canu N. 2006. NMDA receptor mediates tau-induced neurotoxicity by calpain and ERK/MAPK activation. Proc Natl Acad Sci U S A 103(8):2892-2897.

Amadoro G, Serafino AL, Barbato C, Ciotti MT, Sacco A, Calissano P, Canu N. 2004. Role of N-terminal tau domain integrity on the survival of cerebellar granule neurons. Cell Death Differ 11(2):217-230.

Amos LA, Schlieper D. 2005. Microtubules and maps. Adv Protein Chem 71:257-298.

Bell KF, Claudio Cuello A. 2006. Altered synaptic function in Alzheimer's disease. Eur J Pharmacol 545(1):11-21.

Berry RW, Abraha A, Lagalwar S, LaPointe N, Gamblin TC, Cryns VL, Binder LI. 2003. Inhibition of tau polymerization by its carboxy-terminal caspase cleavage fragment. Biochemistry 42(27):8325-8331.

Binder LI, Guillozet-Bongaarts AL, Garcia-Sierra F, Berry RW. 2005. Tau, tangles, and Alzheimer's disease. Biochim Biophys Acta 1739(2-3):216-223.

Bloom GS, Richards BW, Leopold PL, Ritchey DM, Brady ST. 1993. GTP gamma S inhibits organelle transport along axonal microtubules. J Cell Biol 120(2):467-476.

Brady ST. 1985. A novel brain ATPase with properties expected for the fast axonal transport motor. Nature 317(6032):73-75.

Brady ST, Lasek RJ, Allen RD. 1985. Video microscopy of fast axonal transport in extruded axoplasm: a new model for study of molecular mechanisms. Cell Motil 5(2):81-101.

Brandt R, Leger J, Lee G. 1995. Interaction of tau with the neural plasma membrane mediated by tau's amino-terminal projection domain. J Cell Biol 131(5):1327-1340.

Carmel G, Mager EM, Binder LI, Kuret J. 1996. The structural basis of monoclonal antibody Alz50's selectivity for Alzheimer's disease pathology. J Biol Chem 271(51):32789-32795.

Coffey ET, Smiciene G, Hongisto V, Cao J, Brecht S, Herdegen T, Courtney MJ. 2002. c-Jun N-terminal protein kinase (JNK) 2/3 is specifically activated by stress, mediating c-Jun activation, in the presence of constitutive JNK1 activity in cerebellar neurons. J Neurosci 22(11):4335-4345.

Cohen P. 1991. Classification of protein-serine/threonine phosphatases: identification and quantitation in cell extracts. Methods Enzymol 201:389-398.

Drubin DG, Feinstein SC, Shooter EM, Kirschner MW. 1985. Nerve growth factor-induced neurite outgrowth in PC12 cells involves the coordinate induction of microtubule assembly and assembly-promoting factors. J Cell Biol 101(5 Pt 1):1799-1807.

Ebneth A, Godemann R, Stamer K, Illenberger S, Trinczek B, Mandelkow E. 1998. Overexpression of tau protein inhibits kinesin-dependent trafficking of vesicles, mitochondria, and endoplasmic reticulum: implications for Alzheimer's disease. J Cell Biol 143(3):777-794.

Felgner H, Frank R, Biernat J, Mandelkow EM, Mandelkow E, Ludin B, Matus A, Schliwa M. 1997. Domains of neuronal microtubule-associated proteins and flexural rigidity of microtubules. J Cell Biol 138(5):1067-1075.

Ferrer I, Gomez-Isla T, Puig B, Freixes M, Ribe E, Dalfo E, Avila J. 2005. Current advances on different kinases involved in tau phosphorylation, and implications in Alzheimer's disease and tauopathies. Curr Alzheimer Res 2(1):3-18.

Gamblin TC, Berry RW, Binder LI. 2003a. Modeling tau polymerization in vitro: a review and synthesis. Biochemistry 42(51):15009-15017.
Gamblin TC, Berry RW, Binder LI. 2003b. Tau polymerization: role of the amino terminus. Biochemistry 42:2252-2257.
Gamblin TC, Chen F, Zambrano A, Abraha A, Lagalwar S, Guillozet AL, Lu M, Fu Y, Garcia-Sierra F, LaPointe N, Miller R, Berry RW, Binder LI, Cryns VL. 2003c. Caspase cleavage of tau: linking amyloid and neurofibrillary tangles in Alzheimer's disease. Proc Natl Acad Sci U S A 100(17):10032-10037.
Ghoshal N, Garcia-Sierra F, Wuu J, Leurgans S, Bennett DA, Berry RW, Binder LI. 2002. Tau Conformational Changes Correspond to Impairments of Episodic Memory in Mild Cognitive Impairment and Alzheimer's Disease. Exp Neurol 177(2):475-493.
Grant P, Diggins M, Pant HC. 1999. Topographic regulation of cytoskeletal protein phosphorylation by multimeric complexes in the squid giant fiber system. J Neurobiol 40(1):89-102.
Guillozet-Bongaarts AL, Garcia-Sierra F, Reynolds MR, Horowitz PM, Fu Y, Wang T, Cahill ME, Bigio EH, Berry RW, Binder LI. 2005. Tau truncation during neurofibrillary tangle evolution in Alzheimer's disease. Neurobiol Aging 26(7):1015-1022.
Gustke N, Trinczek B, Biernat J, Mandelkow EM, Mandelkow E. 1994. Domains of tau protein and interactions with microtubules. Biochemistry 33(32):9511-9522.
Hayashi S, Toyoshima Y, Hasegawa M, Umeda Y, Wakabayashi K, Tokiguchi S, Iwatsubo T, Takahashi H. 2002. Late-onset frontotemporal dementia with a novel exon 1 (Arg5His) tau gene mutation. Ann Neurol 51(4):525-530.
Horowitz PM, LaPointe N, Guillozet-Bongaarts AL, Berry RW, Binder LI. 2006. N-terminal fragments of tau inhibit full-length tau polymerization *in vitro*. Biochemistry 45(42):12859-12866
.
Horowitz PM, Patterson KR, Guillozet-Bongaarts AL, Reynolds MR, Carroll CA, Weintraub ST, Bennett DA, Cryns VL, Berry RW, Binder LI. 2004. Early N-terminal changes and caspase-6 cleavage of tau in Alzheimer's disease. J Neurosci 24(36):7895-7902.
Jeganathan S, von Bergen M, Brutlach H, Steinhoff HJ, Mandelkow E. 2006. Global hairpin folding of tau in solution. Biochemistry 45(7):2283-2293.
King ME. 2005. Can tau filaments be both physiologically beneficial and toxic? Biochim Biophys Acta 1739(2-3):260-267.
King ME, Ahuja V, Binder LI, Kuret J. 1999. Ligand-dependent tau filament formation: Implications for Alzheimer's disease progression. Biochemistry 38(45):14851-14859.
King ME, Kan HM, Baas PW, Erisir A, Glabe CG, Bloom GS. 2006. Tau-dependent microtubule disassembly initiated by prefibrillar beta-amyloid. J Cell Biol 175(4):541-546.
Kosik KS, Orecchio LD, Binder L, Trojanowski JQ, Lee VM, Lee G. 1988. Epitopes that span the tau molecule are shared with paired helical filaments. Neuron 1(9):817-825.
Kozikowski AP, Gaisina IN, Yuan H, Petukhov PA, Blond SY, Fedolak A, Caldarone B, McGonigle P. 2007. Structure-Based Design Leads to the Identification of Lithium Mimetics That Block Mania-like Effects in Rodents. Possible New GSK-3beta Therapies for Bipolar Disorders. J Am Chem Soc 129(26):8328-8332.
Lee G. 2005. Tau and src family tyrosine kinases. Biochim Biophys Acta 1739(2-3):323-330.

Lee G, Neve RL, Kosik KS. 1989. The microtubule binding domain of tau protein. Neuron 2(6):1615-1624.
Lee G, Thangavel R, Sharma VM, Litersky JM, Bhaskar K, Fang SM, Do LH, Andreadis A, Van Hoesen G, Ksiezak-Reding H. 2004. Phosphorylation of tau by fyn: implications for Alzheimer's disease. J Neurosci 24(9):2304-2312.
Liao H, Li Y, Brautigan DL, Gundersen GG. 1998. Protein phosphatase 1 is targeted to microtubules by the microtubule-associated protein Tau. J Biol Chem 273(34):21901-21908.
Luo MH, Tse SW, Memmott J, Andreadis A. 2004. Novel isoforms of tau that lack the microtubule-binding domain. Journal of Neurochemistry 90(2):340-351.
Morfini G, Pigino G, Beffert U, Busciglio J, Brady ST. 2002a. Fast axonal transport misregulation and Alzheimer's disease. Neuromolecular Med 2(2):89-99.
Morfini G, Pigino G, Brady ST. 2005. Polyglutamine expansion diseases: failing to deliver. Trends Mol Med 11(2):64-70.
Morfini G, Pigino G, Mizuno N, Kikkawa M, Brady ST. 2007a. Tau binding to microtubules does not directly affect microtubule-based vesicle motility. J Neurosci Res.
Morfini G, Pigino G, Opalach K, Serulle Y, Moreira JE, Sugimori M, Llinas RR, Brady ST. 2007b. 1-Methyl-4-phenylpyridinium affects fast axonal transport by activation of caspase and protein kinase C. Proc Natl Acad Sci U S A 104(7):2442-2447.
Morfini G, Pigino G, Szebenyi G, You Y, Pollema S, Brady ST. 2006. JNK mediates pathogenic effects of polyglutamine-expanded androgen receptor on fast axonal transport. Nat Neurosci 9(7):907-916.
Morfini G, Szebenyi G, Brown H, Pant HC, Pigino G, DeBoer S, Beffert U, Brady ST. 2004. A novel CDK5-dependent pathway for regulating GSK3 activity and kinesin-driven motility in neurons. Embo J 23(11):2235-2245.
Morfini G, Szebenyi G, Elluru R, Ratner N, Brady ST. 2002b. Glycogen synthase kinase 3 phosphorylates kinesin light chains and negatively regulates kinesin-based motility. Embo J 21(3):281-293.
Morris JR, Lasek RJ. 1984. Monomer-polymer equilibria in the axon: direct measurement of tubulin and actin as polymer and monomer in axoplasm. J Cell Biol 98(6):2064-2076.
Pigino G, Morfini G, Pelsman A, Mattson MP, Brady ST, Busciglio J. 2003. Alzheimer's presenilin 1 mutations impair kinesin-based axonal transport. J Neurosci 23(11):4499-4508.
Poorkaj P, Muma NA, Zhukareva V, Cochran EJ, Shannon KM, Hurtig H, Koller WC, Bird TD, Trojanowski JQ, Lee VM, Schellenberg GD. 2002. An R5L tau mutation in a subject with a progressive supranuclear palsy phenotype. Ann Neurol 52(4):511-516.
Preuss U, Biernat J, Mandelkow EM, Mandelkow E. 1997. The 'jaws' model of tau-microtubule interaction examined in CHO cells. J Cell Sci 110 (Pt 6):789-800.
Reynolds MR, Lukas TJ, Berry RW, Binder LI. 2006. Peroxynitrite-mediated tau modifications stabilize preformed filaments and destabilize microtubules through distinct mechanisms. Biochemistry 45(13):4314-4326.
Schweers O, Schonbrunn-Hanebeck E, Marx A, Mandelkow E. 1994. Structural studies of tau protein and Alzheimer paired helical filaments show no evidence for beta-structure. J Biol Chem 269(39):24290-24297.

Seitz A, Kojima H, Oiwa K, Mandelkow EM, Song YH, Mandelkow E. 2002. Single-molecule investigation of the interference between kinesin, tau and MAP2c. EMBO Journal 21(18):4896-4905.

Sun W, Qureshi HY, Cafferty PW, Sobue K, Agarwal-Mawal A, Neufield KD, Paudel HK. 2002. Glycogen synthase kinase-3beta is complexed with tau protein in brain microtubules. J Biol Chem 277(14):11933-11940.

Syme CD, Blanch EW, Holt C, Jakes R, Goedert M, Hecht L, Barron LD. 2002. A Raman optical activity study of rheomorphism in caseins, synucleins and tau. New insight into the structure and behaviour of natively unfolded proteins. European Journal of Biochemistry 269(1):148-156.

Vershinin M, Carter BC, Razafsky DS, King SJ, Gross SP. 2007. Multiple-motor based transport and its regulation by Tau. Proc Natl Acad Sci U S A 104(1):87-92.

von Bergen M, Friedhoff P, Biernat J, Heberle J, Mandelkow E. 2000. Assembly of tau protein into Alzheimer paired helical filaments depends on a local sequence motif (306VQIVYK311) forming beta structure. Proc Natl Acad Sci U S A 97(10):5129-5134.

Wang QM, Fiol CJ, DePaoli-Roach AA, Roach PJ. 1994a. Glycogen synthase kinase-3 beta is a dual specificity kinase differentially regulated by tyrosine and serine/threonine phosphorylation. J Biol Chem 269(20):14566-14574.

Wang QM, Roach PJ, Fiol CJ. 1994b. Use of a synthetic peptide as a selective substrate for glycogen synthase kinase 3. Anal Biochem 220(2):397-402.

Yoshiyama Y, Higuchi M, Zhang B, Huang SM, Iwata N, Saido TC, Maeda J, Suhara T, Trojanowski JQ, Lee VM. 2007. Synapse Loss and Microglial Activation Precede Tangles in a P301S Tauopathy Mouse Model. Neuron 53(3):337-351.

FIGURE LEGENDS

Figure 1. Schematic and microtubule binding of tau constructs used in this study. **A)** The longest isoform of tau in the human central nervous system is referred to as hTau40. Boxes represent alternatively spliced exons (E2 and E3), the proline rich region, and the microtubule-binding repeats (R1-R4). Δ2-18 and 1-421 are constructs containing N-terminal and C-terminal deletions, respectively, and K23 is a construct lacking N-terminal exons and microtubule-binding repeats. Tau6P and Tau6D are isoforms that are identical to canonical tau from amino acids 1-144, at which point alternative splicing introduces 11 unique amino acids (represented by dark boxes) followed by a stop codon. The specific amino acids differ between Tau6P and Tau6D. **B)** Tau constructs (5 μM) were incubated with microtubule-containing squid optic lobe cytosol as described in Materials and Methods. Microtubule pellets (P) and supernatant (S) fractions were prepared by centrifugation, and analyzed by immunoblot using antibodies against tau (Tau5) and tubulin. Note that the K23 tau construct lacking MTBRs is mostly recovered in supernatant fractions, consistent with its weak binding to microtubules. In contrast, hTau40 is recovered in association with microtubules. Neither construct was recovered in pellet fractions when centrifuged in the absence of squid microtubules (data not shown).

Figure 2. The effect of hTau40 on the morphology of axoplasmic squid microtubules. **A)** After perfusion of squid axoplasm with control buffer, individual microtubules can be observed at the axoplasm periphery. Many of these microtubules display a gently curving, freely bending morphology (white arrows). **B)** Perfusion of hTau40 at 2 μM dramatically changes the morphology of peripheral microtubules to a stiff, linear appearance (white arrows). This effect of tau and other MAPs on microtubule stiffness has been previously characterized in vitro (Felgner

et al. 1997), and indicates direct binding of hTau40 to endogenous squid microtubules. **C)** In contrast to monomeric hTau40, perfusion of filamentous hTau40 at 2 μM does not change the morphology of peripheral microtubules.

Figure 3. Effects of soluble and filamentous tau on FAT. Axoplasms were perfused with soluble or filamentous recombinant tau (hTau40), and FAT rates (μm/sec) monitored over a period of 50 min. Each arrowhead represents a measurement of the average velocity at which particles move in the anterograde (►) or retrograde (◄) direction. Graphs depict compiled data from at least three separate trials. While soluble hTau40 (2 μM) had no observable effect on either FAT direction **(A)**, hTau40 filaments (2 μM) specifically inhibited anterograde FAT in a time-dependent manner **(B)**.

Figure 4. Characterization of tau filaments. Tau constructs hTau40, Δ2-18, and 1-421 were all recognized by Western blot analysis with the antibody Tau5, which recognizes an epitope near the middle of the protein (top panel). Δ2-18 is not recognized by the N-terminal antibody Tau12, and the C-terminal antibody Tau46.1 does not recognize 1-421 (lower panel) **(A)**. Filaments generated from 4 μM hTau40 **(B)**, Δ2-18 **(C)**, and 1-421 **(D)** following five hours of polymerization with arachidonic acid. Fixed samples were negatively stained and viewed by electron microscopy. Representative digital micrographs are shown. Size bars represent 200 nm.

Figure 5. Removal of the extreme N-terminus of tau abolishes the effects of tau filaments on FAT. Box plots of FAT rates in axoplasm perfused with 2 μM soluble or filamentous tau. Data

represent pooled measurements taken between 30 and 50 min of observation. Perfusion with filaments composed of hTau40 (hTau40 F) and 1-421 (1-421 F) significantly reduced anterograde FAT compared to hTau40 monomer (hTau40 M) rate at (*$p \leq 0.0001$ by a 2 sample t test). In contrast, Δ2-18 filaments (Δ2-18 F) failed to inhibit anterograde FAT **(A)**. Retrograde FAT was unaffected in all conditions **(B)**. Rates for monomeric hTau40 were indistinguishable from axoplasm perfused with buffer alone (data not shown).

Figure 6. The N-terminus of tau is sufficient to inhibit anterograde FAT. Graph representing pooled data from axoplasms perfused with either Tau6P or Tau6D (2 μM). The N-terminus of both isoforms is identical to that of hTau40, but they lack the MTBR region and the C-terminus. When perfused as monomer into isolated axoplasm, these isoforms inhibit anterograde FAT. The effect was not statistically different from inhibition caused by hTau40 filaments.

Figure 7. The effect of tau filaments is mediated by the activity of GSK-3. Co-perfusion of hTau40 filaments with phospho-CREB peptide (0.5 mM), a competitive inhibitor of GSK-3, blocked the effects of hTau40 filaments on FAT (**A**). The inhibitory effect of tau filaments on FAT was also blocked by co-perfusion with another specific GSK-3 inhibitor, ING-135 (100 nM; **B**). SB203580 (5 μM), a stress-activated protein kinase inhibitor, did not prevent the effects of hTau40 filaments on FAT (**C**). Perfusion of any of these inhibitors alone showed no effect on FAT (data not shown).

Figure 8. Perfusion of active GSK-3β or filamentous tau induces kinesin-1 release from squid vesicle fractions. **(A)** Purified vesicle fractions from individual axoplasms perfused with buffer

control or active GSK-3β, and with soluble tau or filamentous tau were immunobloted for kinesin-1 heavy chain (KHC), dynein intermediate chain (DIC) and SNAP-25 antibodies. Note the dramatic reduction of kinesin-1 from membrane fractions of axoplasms perfused with GSK-3β and filamentous tau. **B)** Perfusion of active GSK-3β and filamentous tau reduces kinesin-1 membrane association by ≅ 50%. Membrane binding values of KHC, DIC and SNAP-25 are expressed as the ratio between axoplasms perfused with active GSK-3β over buffer control and fibrillar over soluble tau. Values were obtained by using the Image J software from NIH and represent the mean ± SEM from three independent experiments. The difference between soluble and filamentous tau was significant at $p \leq 0.05$ using a two sample t-test of $\mu 1 - \mu 2$.

Figure 9. The effect of tau filaments depends upon PP1 activity. The inhibitory effect of tau filaments on FAT was blocked by co-perfusion with **(A)** the serine-threonine phosphatase inhibitor okadaic acid (100 nM), and **(B)** the PP1-specific inhibitor I-2 (50 nM). Perfusion of either of these inhibitors alone had no effect on FAT (data not shown).

Figure 10. Proposed mechanism underlying tau filament-induced inhibition of anterograde FAT. Pharmacological experiments presented here indicate that FAT inhibition requires the activity of PP1 and GSK-3. We have previously described a pathway in which PP1 dephosphorylates and activates GSK-3, which subsequently phosphorylates kinesin light chains (KLCs). Phosphorylation of KLCs, promotes a chaperone-mediated detachment of kinesin-1 from its transported cargo. Our results suggest that tau can trigger this cascade when the amino terminus of tau is abnormally exposed in the filamentous form.

Supplemental Figure 1. The effect of 1-421 tau filaments is mediated by the activity of GSK-3. Axoplasms were perfused with filaments of 1-421 tau, and FAT rates (μm/sec) monitored over a period of 50 min. (A) Perfusion of 1-421 filaments (2 μM) specifically inhibited anterograde FAT in a time-dependent manner much as seen with filaments made from full-length tau ht40. (B) Co-perfusion of 1-421 filaments with phospho-CREB peptide (0.5 mM), a competitive inhibitor of GSK-3, blocked the effects of 1-421 filaments on FAT. These data indicate that the effects of 1-421 filaments on anterograde FAT are also mediated by activation of GSK-3. Graphs depict compiled data from at least three separate trials.

Supplemental Figure 2. Rendering of **5-ING-135** in complex with GSK-3β. This complex structure was generated from the available x-ray structure of the protein co-crystallized with staurosporine (PDB:1Q3D) with docking of the inhibitor performed using Molegro Virtual Docker program. ING-135 is a derivative of the natural product staurosporine that binds to the ATP-binding site of GSK-3, exhibiting an IC_{50} of 7nM.

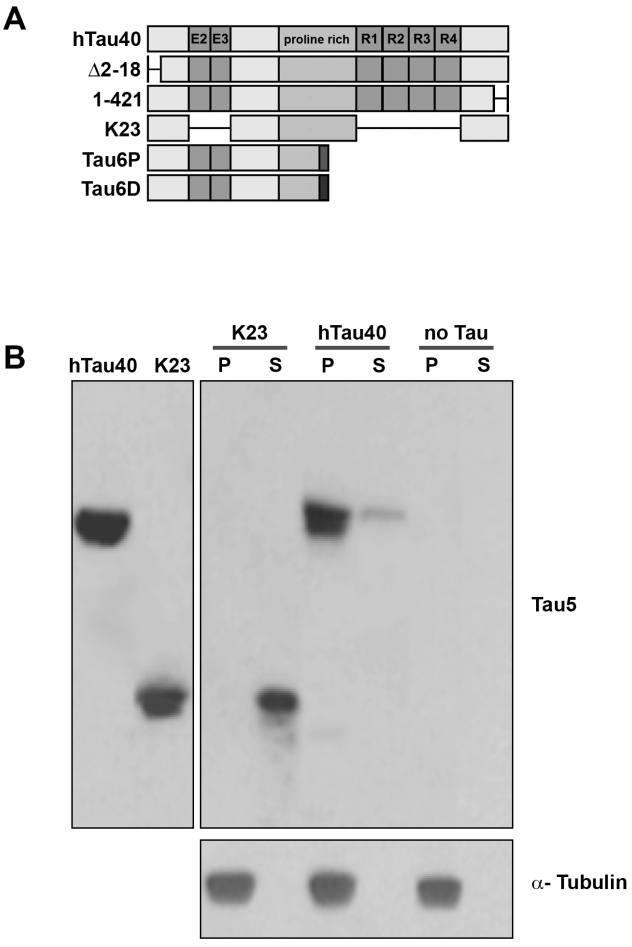
A
hTau40
E2
E3
proline rich
R1
R2
R3
R4
Δ2-18
1-421
K23
Tau6P
Tau6D
B
K23
hTau40
no Tau
hTau40
K23
P
S
P
S
P
S
Tau5
α- Tubulin

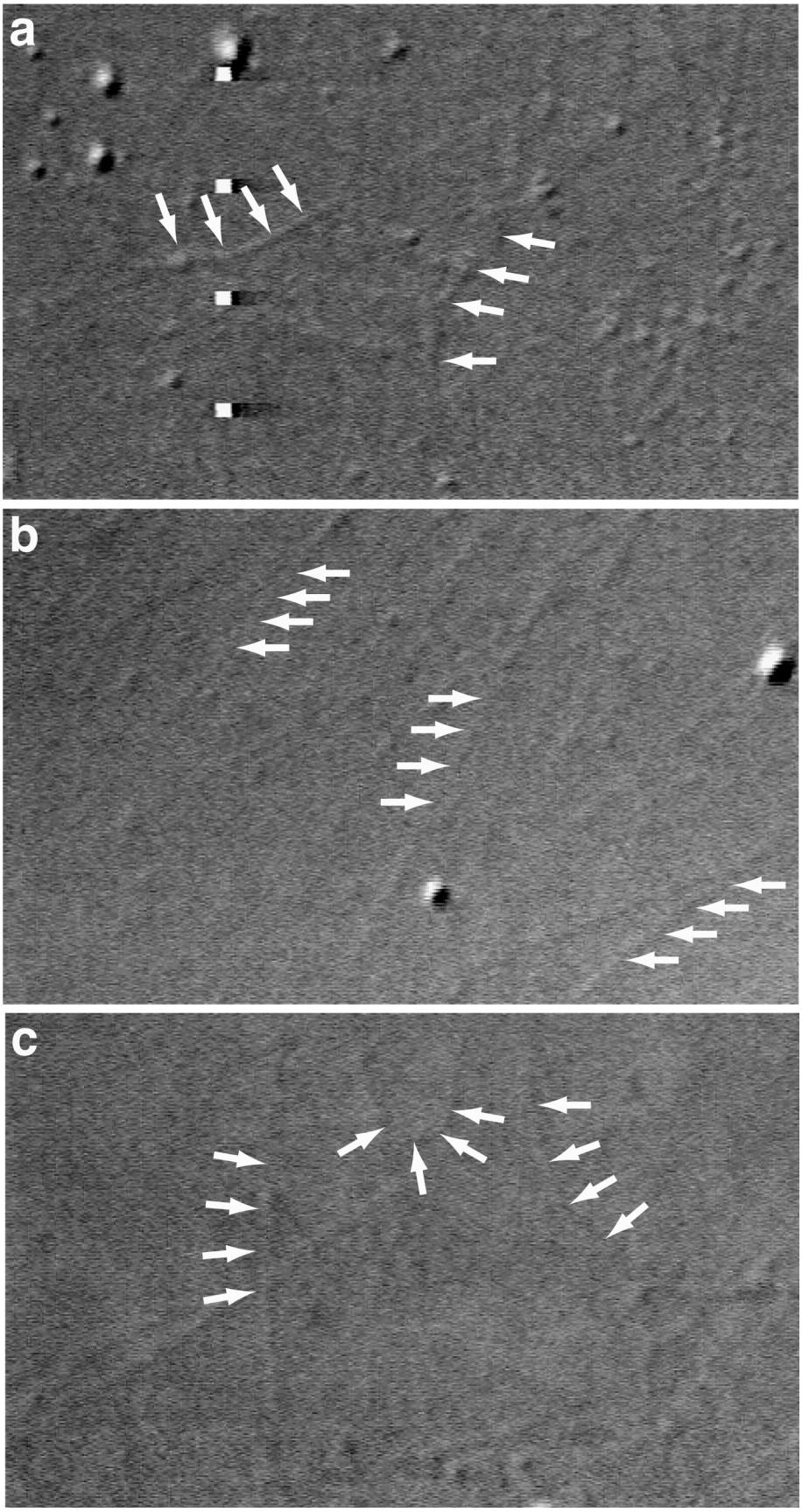
a
b
c

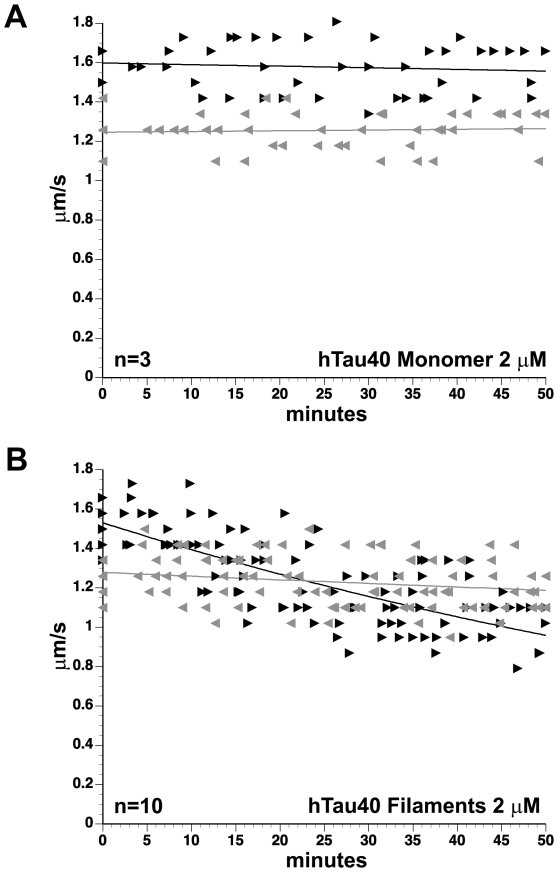
A
1.8
1.6
1.4
1.2
1
0.8
0.6
0.4
0.2
0
μm/s
n=3
hTau40 Monomer 2 μM
0
5
10
15
20
25
30
35
40
45
50
minutes
B
1.8
1.6
1.4
1.2
1
0.8
0.6
0.4
0.2
0
μm/s
n=10
hTau40 Filaments 2 μM
0
5
10
15
20
25
30
35
40
45
50
minutes

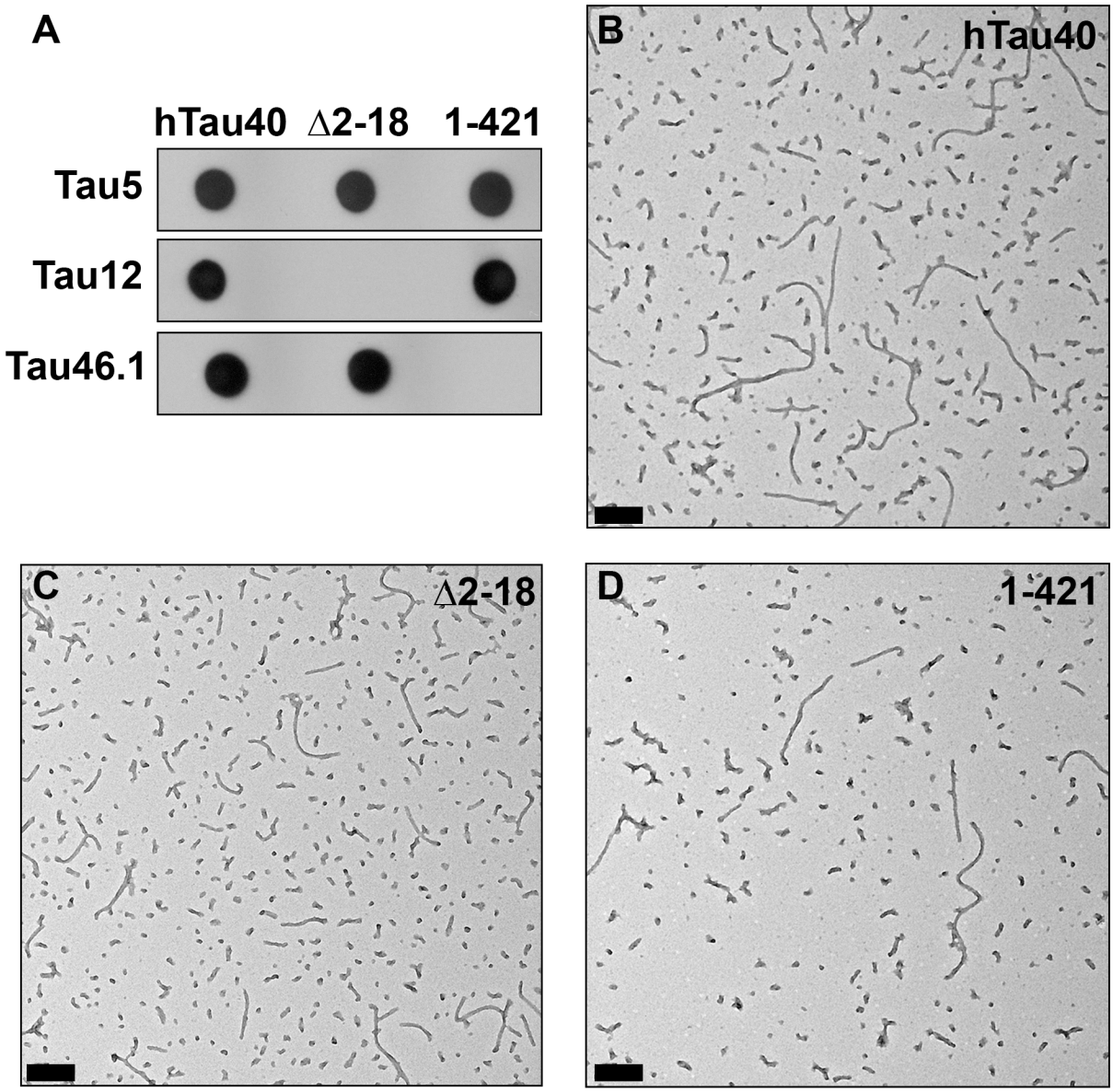
A
hTau40
Δ2-18
1-421
Tau5
Tau12
Tau46.1
B
hTau40
C
Δ2-18
D
1-421

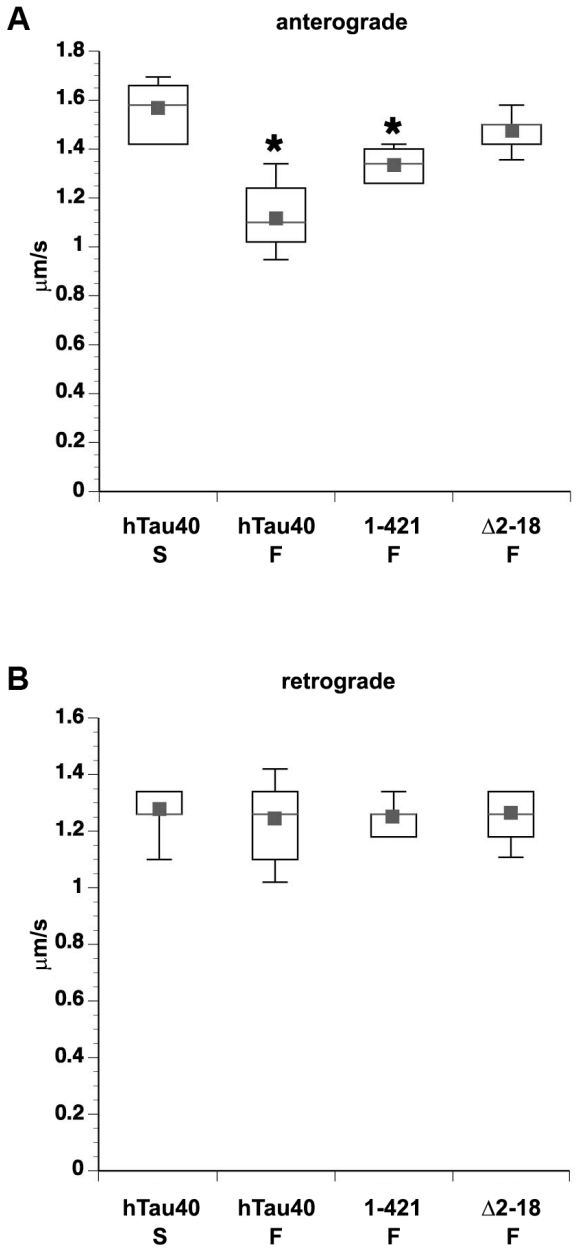
A
anterograde
1.8
1.6
1.4
1.2
1
0.8
0.6
0.4
0.2
0
µm/s
*
*
hTau40 S
hTau40 F
1-421 F
Δ2-18 F
B
retrograde
1.6
1.4
1.2
1
0.8
0.6
0.4
0.2
0
µm/s
hTau40 S
hTau40 F
1-421 F
Δ2-18 F

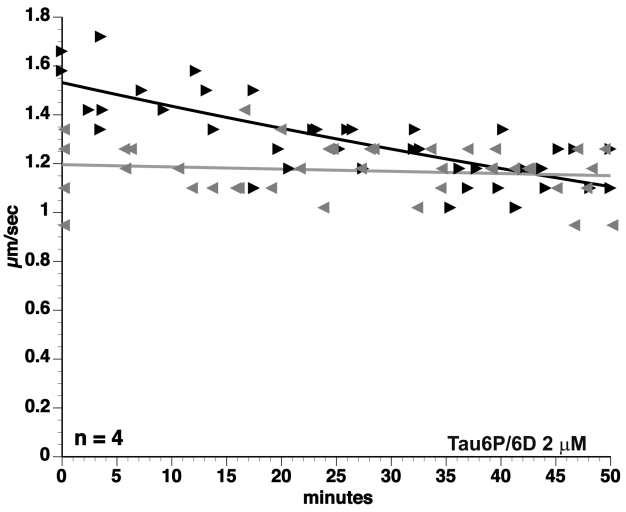
1.8
1.6
1.4
1.2
1
0.8
0.6
0.4
0.2
0
µm/sec
n = 4
Tau6P/6D 2 µM
0
5
10
15
20
25
30
35
40
45
50
minutes

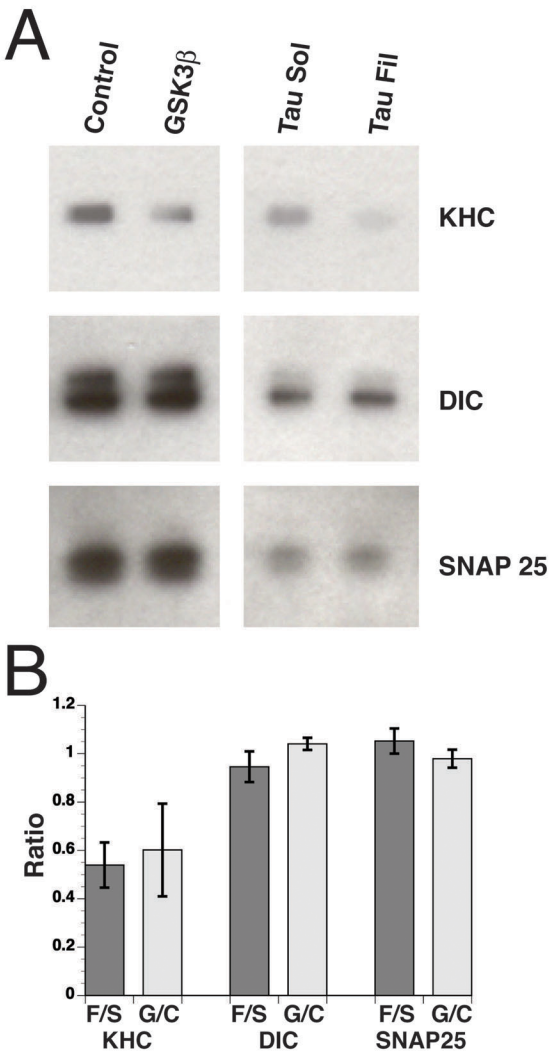
A
Control
GSK3β
Tau Sol
Tau Fil
KHC
DIC
SNAP 25
B
Ratio
1.2
1
0.8
0.6
0.4
0.2
0
F/S
G/C
KHC
DIC
SNAP25

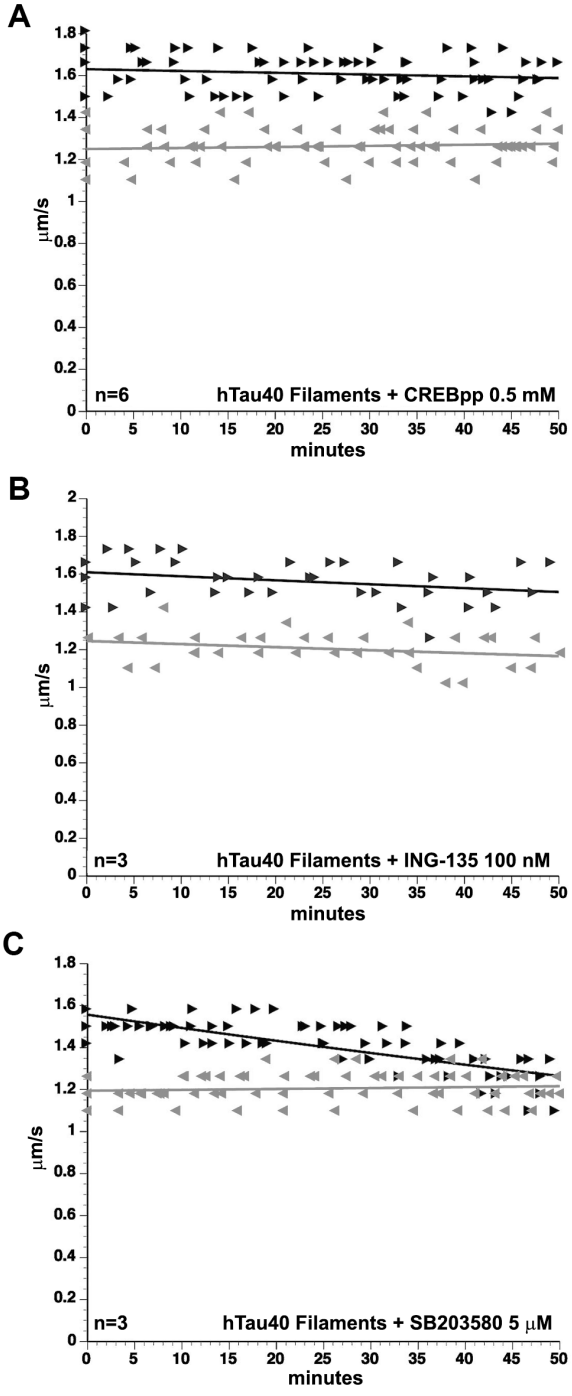
A
μm/s
n=6
hTau40 Filaments + CREBpp 0.5 mM
minutes
B
μm/s
n=3
hTau40 Filaments + ING-135 100 nM
minutes
C
μm/s
n=3
hTau40 Filaments + SB203580 5 μM
minutes

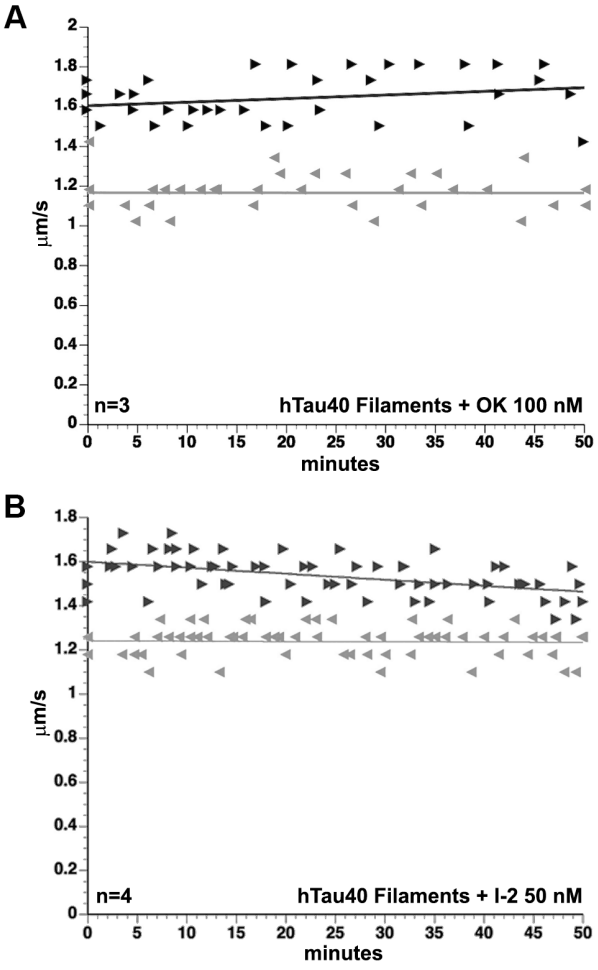
A
μm/s
n=3
hTau40 Filaments + OK 100 nM
minutes
B
μm/s
n=4
hTau40 Filaments + I-2 50 nM
minutes

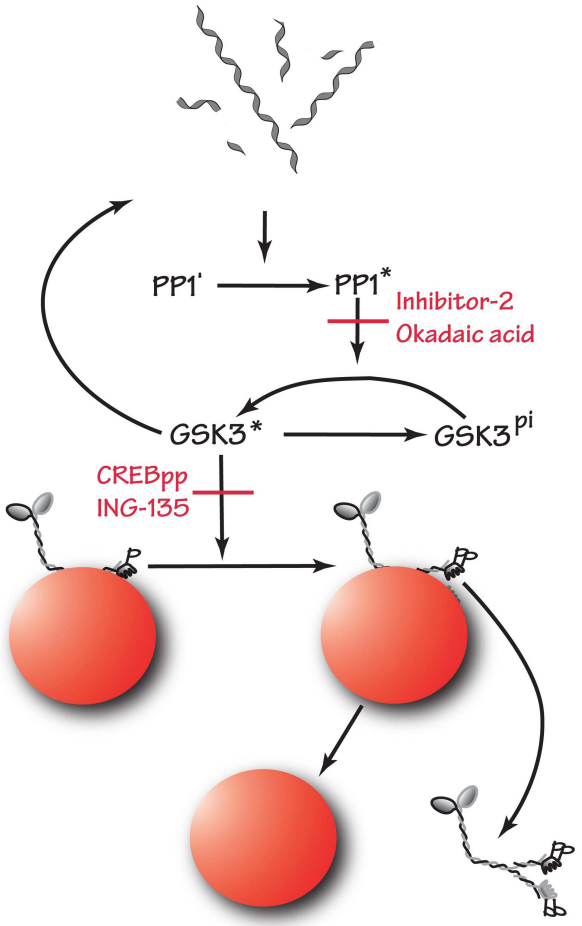
PP1'
PP1*
Inhibitor-2
Okadaic acid
GSK3*
GSK3pi
CREBpp
ING-135
P
P
P

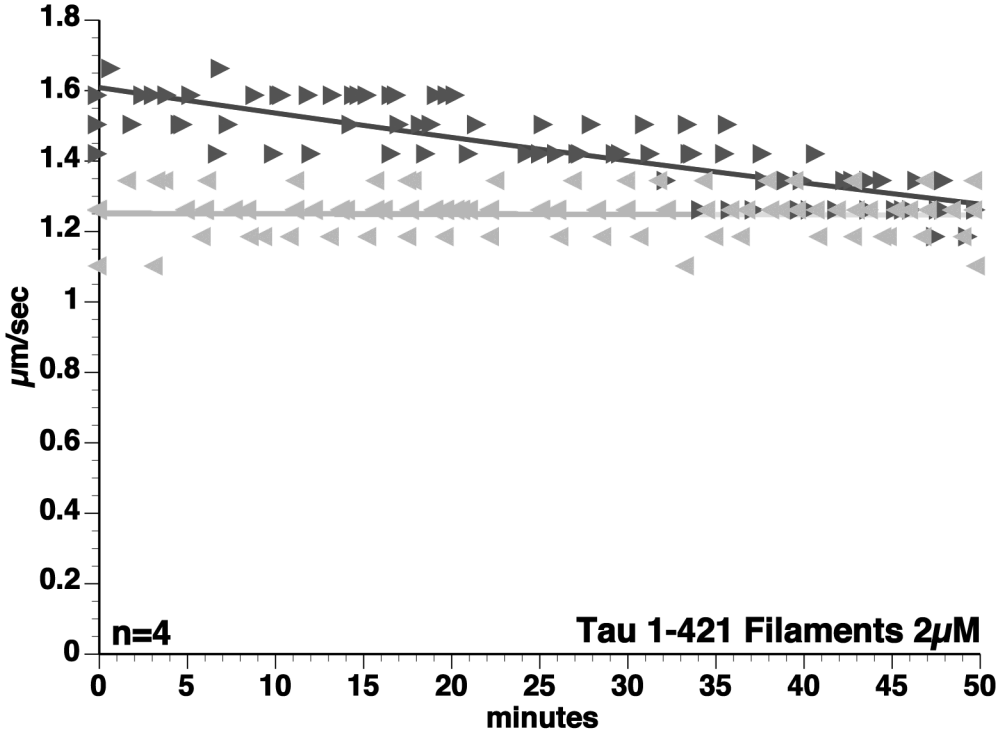
1.8
1.6
1.4
1.2
1
0.8
0.6
0.4
0.2
0
µm/sec
n=4
Tau 1-421 Filaments 2µM
0
5
10
15
20
25
30
35
40
45
50
minutes

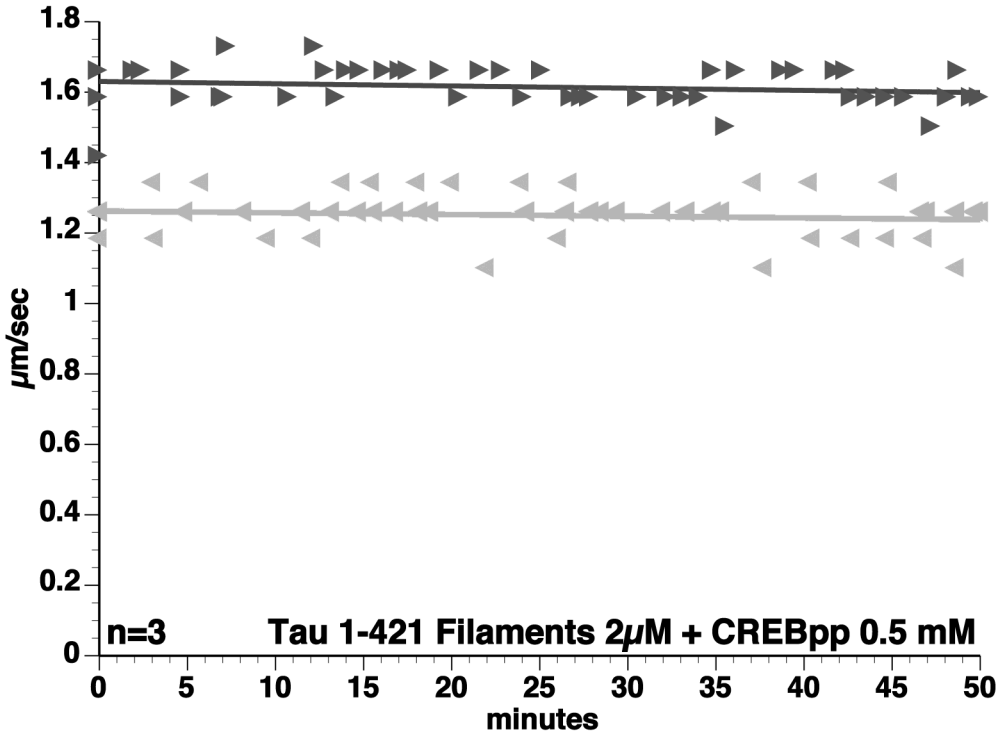
1.8
1.6
1.4
1.2
1
0.8
0.6
0.4
0.2
0
µm/sec
n=3
Tau 1-421 Filaments 2µM + CREBpp 0.5 mM
0
5
10
15
20
25
30
35
40
45
50
minutes